Title

Loss of Disabled-1 Reduces Olfactory Adult Neurogenesis

Author

Zimmer, Samantha

Publication Date

2022

Peer reviewed|Thesis/dissertation

UNIVERSITY OF CALIFORNIA

Los Angeles

Loss of Disabled-1 Reduces Olfactory Adult Neurogenesis

A thesis submitted in partial satisfaction

of the requirements for the degree Master of Science

in Physiological Science

by

Samantha Zimmer

2022

ABSTRACT OF THE THESIS

Loss of Disabled-1 Reduces Olfactory Adult Neurogenesis

by

Samantha Zimmer

Master of Science in Physiological Science

University of California, Los Angeles 2022

Professor Patricia Phelps, Chair

This study examines the role of the Reelin-signaling pathway in the peripheral olfactory system. We found that olfactory sensory neurons (OSNs) express the Disabled-1 (Dab1) protein and *Dab1* mutants have reduced olfactory detection compared to controls. We generated a conditional deletion of *dab1* in OSNs. We studied differences in OSN neurogenesis by comparing the number of immature neurons marked by GAP43 in our no-cre controls to *OMP*-cre; *Dab1 flox/flox* and *OMP-cre*; *Dab1 flox/+* mice. *OMP-cre*; *Dab1 flox/flox* mice had fewer GAP 43-labeled cells compared to the no-cre controls. The reduction in immature OSNs prompted us to explore the number of olfactory stem cells and proliferative cells by localizing *Sox2* and *Ki67*, respectively. We found that the *OMP-cre*; *Dab1 flox/flox* mice had many fewer *Sox2* and *Ki67*-expressing cells in their olfactory epithelium (OE) than control mice. This work

reveals that *dab1* is critical for adult neurogenesis within the OE.

The thesis of Samantha Zimmer is approved.

Xian-Jie Yang

Mark Frye

Patricia Phelps, Committee Chair

University of California, Los Angeles

ACKNOWLEDGEMENTS

First and foremost, I would like to thank Dr. Patricia Phelps for serving as my mentor over the last five years. Dr. Phelps is the embodiment of hard-work, integrity, and dedication. She is and always will be my role model.

I would also like to thank my former mentor, SunYoung Lee, for helping me build my basic wet lab skills and producing critical data that inspired this project.

Next, I would like to acknowledge Mahlet Mekonnen for supporting me along every step of my project and providing me with the best company to do research alongside. I am especially grateful for my three undergraduate mentees, Jasmine Louie, Isabella Hayes-Velasco, and Netpheel Wang, for their willingness and excitement to learn. To all the members of the Phelps's lab, thank you for making me laugh and excited to come into lab each day.

Lastly, I would like to acknowledge my incredible parents. To my Mom, who has given me endless love and encouragement—I would not have made it this far without you. To my Dad, thank you for all that you've provided to our family and always brightening up my day when life gets heavy.

TABLE OF CONTENTS

LIST OF FIGURES

Introduction

The mammalian olfactory system is responsible for odor detection and discrimination. The major component of the peripheral olfactory system is the olfactory epithelium. Embedded within the olfactory epithelium are olfactory sensory neurons (OSNs), which are responsible for odorant detection. Olfactory receptor genes are the largest and most diverse mammalian gene family (Buck and Axel, 1999). Each olfactory sensory neuron expresses a single olfactory receptor out of the approximately 1,100 functional olfactory receptor genes and projects to specific glomeruli in each of the olfactory bulbs (Chess *et al.*, 1994; Clowney *et al.*, 2012). These OSNs die, and are replaced throughout life and therefore exist in both immature and mature forms in the adult olfactory epithelium (OE). Within 12 days, mouse OSNs are generated from basal progenitor cells and develop into their mature form with axons reaching their glomerular targets (Liberia *et al*., 2019).

The lifelong capacity for neurogenesis of OSNs is the result of stem cells situated at the basal position of the olfactory epithelium. The horizontal basal cells (HBCs) and globose basal cells (GBCs) are thought to serve different functions in maintaining the various cell types of the OE. HBCs have a flattened appearance, adhere to the basal lamina of the OE, and are mitotically quiescent in an uninjured OE. The HBCs divide approximately every 60 days (Schwob *et al*., 2017), act as a stem cell reserve in the case of injury (Holbrook *et al.*, 1995; Carter *et al.*, 2004), and generally do not contribute to the differentiation of neuronal or non-neuronal cells found in the OE. These multipotent stem cells, however, have the capability of giving rise to all the cell types of the OE, including the OSNs, sustentacular cells, and globose basal cells (Leung, 2007). HBCs are identified by their expression of Transformation related protein 63 (Trp63), a transcription factor that contributes to maintaining the multipotency of these progenitor cells. In

lesion experiments that involve substantial damage to the neuronal and non-neuronal cells of the OE, Trp63 is downregulated and their multipotency is activated (Packard *et al*., 2011).

The GBCs are the second type of olfactory stem cell and they are found between the OSNs and the HBCs. These progenitor cells express a defined sequence of transcription factors during neurogenesis that mark distinct stages in OE cell type differentiation in both embryos and adults (Nicolay *et al.,* 2006). Unlike the mostly quiescent HBCs, GBCs display a high proliferative rate, dividing almost every day in order to maintain cells found within the OE (Mackay-Sim and Kittel, 1991; Huard and Schwob, 1995). GBCs are first identified by their expression of transcription factor *Sox2* and then take on heterogeneous morphologies and functions within the OE. Proliferative GBCs also are distinguished from quiescent GBCs by their expression of *Ki67* (Gerdes *et al.,* 1984). Once committed to a cell type, GBCs begin to express the early neuronal marker *Ascl1*, which is followed by expression of *Neurogenin1* and *NeuroD1* in immediate neuronal progenitor cells (Cau, 1997). Additionally, GBCs can express markers for the non-neuronal sustentacular cells, such as *Hes1* (Manglapus *et al*., 2004). GBCs are responsible for the continuous generation of OSNs throughout life.

Depending on their level of maturation, OSNs vary in their locations within the olfactory epithelium (Buck and Axel, 1999). Immature OSNs are found next to the stem cells, at the base of the olfactory epithelium. Immature OSNs, many of which have yet to extend their cilia, are identified by their expression of Growth Associated Protein 43 (GAP 43; Verhaagen et al., 1989). GAP43 impacts neuronal plasticity and growth and a reduction of GAP43 expression is associated with defects in axon guidance and neuronal development (Strittmatter *et al*., 1995). By contrast, a mature OSN is a bipolar neuron with a dendrite ending in twelve or more mucus-covered cilia that project into the nasal cavity, and a single, unbranched axon that courses from

the OE into the cranial cavity (Farbman, 1992; Mombaerts, 2001). Mature OSNs are identified by olfactory marker protein (OMP), and are found throughout the main olfactory epithelium (Farbman and Margolis, 1980). Olfactory marker protein expression increases with glomerular innervation and is suggested to play a key role in the final axonal targeting and synaptogenesis (Farbman and Margolis, 1980).

There is a unique type of glia associated with the olfactory system – olfactory ensheathing cells (OECs). After OSNs are generated from the basal stem cell layer in the olfactory epithelium, they project their axons into the lamina propria where they are surrounded by OECs. Their axons then gather into fascicles and form the olfactory nerve, course through the cribriform plate into the olfactory nerve layer, and finally synapse within the glomerular layer of the olfactory bulb. The OSN axons are surrounded by OECs until they enter into the glomerulus, the site where they synapse on mitral cell targets (Klenoff and Greer, 1998). These singular projections contribute to a glomerular map of the many different olfactory receptors.

This project focuses on the role of the Reelin-signaling pathway within the mammalian peripheral olfactory system. Reelin is a secreted glycoprotein that binds both the apolipoprotein E receptor 2 (Apoer2) and the very-low-density lipoprotein receptors (Vldlr; D'Arcangelo *et al*., 1999). The binding activates the Src-family kinases and phosphorylation of the intracellular adaptor protein Disabled-1 (Dab1). Dab1 and Reelin mutants have mispositioned neurons in the central nervous system due to migratory errors during development (Howell *et al*., 1997; Rice *et al.*, 1998). Reelin, Dab1 and Vldlr have been shown to be expressed within the peripheral olfactory system (Zikova *et al*., 2009; Dairaghi *et al*., 2018). We found that OSNs express Dab1 and OSNs undergo continuous neurogenesis throughout the lifetime of an organism. Thus, we

suspect that the loss of the Reelin-Dab1 signaling pathway may also regulate olfactory neurogenesis.

In this study, we want to determine whether or not *dab1* influences adult neurogenesis in the OE. Recent unpublished data from our lab showed that OSNs express Dab1, OECs secrete Reelin, and *Reelin*$^{-/-}$ and *Dab1*$^{-/-}$ mice have reduced olfactory detection compared to wild type mice. To test if their olfactory dysfunction was due to changes in the OSNs, we generated a tissue specific deletion of *Dab1* (*OMP-cre; Dab1 flox/flox; Ai14* and the *OMP-cre; Dab1 flox/+; Ai14*) and no-cre controls. We then asked if the reduction of *Dab1* influenced OSN neurogenesis by examining the number of GAP43-labeled OSNs in the conditional *Dab1*$^{+/-}$ and *Dab1*$^{-/-}$ mice and the controls. We also asked if the removal of *dab1* affected the olfactory stem cell population, i.e., the OSN progenitors. By examining the number and distribution pattern of newly differentiated immature OSNs and olfactory stem cells, we will determine if the loss of *dab1* in OMP-expressing cells affects adult neurogenesis in the OE.

Materials and Methods

Animals:

To confirm that the TdTomato faithfully reproduced the OMP expression, we generated a mouse line by crossing the *OMP-cre* mouse (Jackson Laboratory, stock #000668, Bar Harbor, ME, Li et al., 2004) with an *Ai14 TdTomato* (*TdTom*, Jackson Laboratory, Bar Harbor, ME, stock #007908, Madisen et al., 2010) reporter mouse.

To determine the contribution of Dab1 in the peripheral olfactory system to the olfactory circuit, we generated a male cre driver and a female Ai14 (TdTom) reporter mouse. To obtain the male cre driver, we bred an *OMP-cre/+* mouse with a *Dab1-flox/Dab1-flox* mouse (Gift from Dr.

Brian Howell; Suny Upstate Medical University, Syracuse, NY) to obtain the *OMP-cre; Dab1-flox*/+ mice and genotyped according to the protocol in Pramatarova *et al.* (2007); Abadesco *et al*., (2014). To generate the female *Ai14* (TdTom) reporter mouse, we bred the *Dab1-flox/Dab1-flox* with an *Ai14/Ai14* mouse. The first generation of offspring were then crossed again with their parental mouse line to produce a female with the desired genotype of *Dab1-flox/Dab1-flox*, *Ai14/Ai14*. The final cross to produce a conditional Dab1 mouse was to breed the cre driver (*OMP-cre; Dab1-flox/*+) and the Ai14 reporter (*Dab1-flox/Dab1-flox*, *Ai14/Ai14*), which produced the following 4 genotypes: 1) *OMP-cre; Dab1 flox/+; Ai14/+, 2*) *OMP-cre*; *Dab1 flox*/*flox*; *Ai14/*+, 3) no-cre; *Dab1 flox/*+; *Ai14/*+, and 4) no-cre; *Dab1 flox*/*flox*; *Ai14/*+. In this paper, we use the acronym "ODA", underlined in genotype 1 above, to refer to our triple cross mouse. Because all four genotypes are *Ai14/*+, we will use the following abbreviations: *OMP-cre; Dab1 f/*+, no-cre; *Dab1 f/+, OMP-cre; Dab1 f/f*, and no-cre; *Dab1 f/f.* Tail DNA was collected, genotyped using polymerase chain reaction according to their specified protocol, and the results were amplified by gel electrophoresis.

Tissue Collection and Preparation:

For anatomic analyses, adult mice who were 3-6 months old of either sex were deeply anesthetized with Pentobarbital (80 mg/kg). Once deeply sedated, the chest was opened, and the mouse was perfused through the heart with 4% paraformaldehyde fixative in 0.12 M Millonig's Phosphate buffer for 10 min. Following the perfusion, the head was removed and postfixed for 1 hr in the same fixative at 4°C, washed in Millonig's Buffer multiple times, and stored in 0.12M Millonig's with Azide (0.06%). The soft tissues of the head and jaw were removed before the head underwent a decalcification process. After washing with double-distilled, sterile ultrapure water for 3 mins, the heads were placed in an undiluted formic acid bone decalcifier

(Immunocal, Decal Chemical Corps, Tallman, NY) for 8 hrs. Heads were washed again in double-distilled water for 3 mins and stored in 0.12M Milloning's buffer with 0.06% Azide. Before sectioning, the heads were placed in a series of increasing concentration of sucrose: 5%, 10%, and 15% sucrose in Milloning's buffer for 20 mins on the rotator at room temperature, and then placed in 20% sucrose and stored at 4°C on the rotator overnight. The following day, the heads in 20% sucrose were heated to 37°C for 1.5 hrs. The heads were infiltrated with a 20% gelatin-sucrose mixture for 4 hrs, embedded in plastic molds, frozen on dry ice, and stored at -70°C.

Immunofluorescence:

To evaluate OMP expression, the nasal cavity and olfactory bulb were sectioned 25 μm thick in the coronal plane using a cryostat, and slide mounted on a series of sixteen slides (Thermo Fisher Scientific, 3039). Each slide contained about 6 sections throughout the anterior-posterior extent of the olfactory system. To identify mature olfactory sensory neurons, immunofluorescence was carried out to examine the expression of Olfactory Marker Protein (OMP). Sections were rinsed with Phosphate-buffered saline (PBS) 3X with a 10-min incubation between each wash, treated with a presoak of 1% hydrogen peroxide and PBS for 15 mins, and then placed in 1% Triton-X100 (TX. Sigma-Aldrich) for 30 mins followed by a 1 hr incubation in 30% normal donkey serum (NDS) and 0.4% TX. We incubated sections in goat anti-OMP antibodies (1:1000, FujifilmWako, 544-10001-WAKO, Richmond, VA) with 5% TX, 5% NDS, and PBS buffer at room temperature overnight. The following day sections were washed 3X with PBS buffer. The secondary antibody, donkey anti-goat 488 (1:250, Jackson ImmunoResearch, West Grove, PA), was diluted in PBS and incubated with sections for 1 hr. Sections were washed well and coverslipped with Fluorogel (Electron Microscopy Sciences, Hatfield, PA).

We also localized GAP43 expression in order to identify immature OSNs. These slide-mounted sections were rinsed with PBS 3X for 10 min each. Next, the slide was placed in normal serum (2% NDS, 2% BSA Albumin, and 0.25% TX in PBS) for 1 hr. We used rabbit anti-GAP43 (1:500, Abcams, ab16053, Cambridge, MA) diluted in normal serum and incubated for 2 days at RT with sections stored overnight at 4°C. The following day the slides were washed 3X with PBS buffer. The secondary antibody donkey anti-rabbit 488 (1:250, Thermo Fisher Scientific, Waltham, MA) was diluted in PBS buffer and incubated for 2 hrs. Sections were washed again and coverslipped. TdTom fluorescence was strong enough to image without further amplification.

To detect Sox2 and Ki67 in adult OE sections, we used the Tyramide Signal Amplification (TSA) kit to localize olfactory stem cells and proliferating olfactory progenitors, respectively. Slides containing OE were first rinsed with Tris-buffered saline with BSA (TBS-BSA). Next, slides were incubated in a pre-soak comprised of 1% H_2O_2 , 0.1% sodium azide, and TBS-BSA. Slides were rinsed in TBS-BSA, and then soaked in a blocking serum for 1 hr (5% NDS and 0.1% TX in TBS-BSA). Slides are then placed in Avidin (1:1; Vector Laboratories, SP-2001) and Biotin (1:1; Vector Laboratories, SP-2001). Sections were incubated in rabbit anti-Sox2 (B3, 1:5000; Abcams, ab92494) or rabbit anti-Ki67 (Abcams, ab16667) overnight. On day 2, slides were rinsed with TBS-BSA 3 times. Next, slides were incubated in biotinylated donkey anti-rabbit IgG (1: 1,000, Life Technologies, A21206) in Tris-NaCl-Block (TNB) buffer. Sections are then rinsed twice in Tris-NaCl-Tween (TNT) buffer, which is then followed by soaking slides in streptavidin- conjugated horseradish peroxidase (1:500, Perkin Elmer LLC, NEL750001EA) in TNB. Sections were incubated in TSA-plus Fluorescein (1:150; Perkin Elmer

LLC, NEL741001KT) in 1x Plus Amplification Diluent (Perkin Elmer, FP1498) for 10 mins. Slides were rinsed twice using TNT, and left to dry before sections were coverslipped using Fluorogel. A summary table of the primary and secondary antibodies used in our analyses are found in the supplemental section (Supplemental Fig. 1).

Microscopy

We used a Zeiss Laser Scanning Microscope (LSM800) to obtain high resolution confocal images of the OE for our analyses of GAP43, Sox2, and Ki67 expression. High magnification images were taken using the 40x oil immersion lens with the pinhole aperture set to 1 Airy unit. Optical slices were obtained using the laser with a wavelength of 488 nm. When capturing the image, we scanned through 10-12 µm of z-stacks to determine the region of the OE that contained the largest number of immunolabeled cells. Confocal images contained 3-6 z-stacks, and the optical slice with the highest number of immunoreactive cells were analyzed.

Low-magnification images were obtained using an Olympus AX70 microscope. The images were processed using Zeiss Zen computer software (2012).

Experimental design:

To determine if Growth Associated Protein 43 (GAP43) expression is limited to immature OSNs, we examined several sections of OE from three *OMP-cre*; Ai14+/- mouse to determine if there were OSNs that co-expressed the OMP genetic marker and GAP43 immunohistochemistry. We performed only a qualitative analysis on these sections.

To analyze GAP43 expression in the OE in the 4 ODA genotypes, we took single optical slices along the dorsal nasal septum within a 72 µm by 414 µm rectangle**.** For our GAP 43 analysis there were 5-8 mice examined/genotype: *OMP-cre; Dab1 f/+* (n= 5), *OMP-cre*; *Dab1 f/f* (n= 6), and no-cre control groups (no cre; *Dab1 f/+;* no cre; *Dab1 f/f;* n= 8). Confocal images

(40X) of GAP43-labeled cells were obtained from 1 anterior and 1 posterior slice/mouse. We counted GAP43 cells in the rectangular box of a single optical slice/section and used the z-stack only to confirm the GAP43-labeled cellular identity. To be included in this analysis, the entire cell body and at least part of the dendritic process was found within the single optical slice. GAP43-labled cells were analyzed by two independent evaluators, one of whom was blind to the genotype. The independent counts for each section were averaged, the mean per animal calculated and then the average of the animals in each genotype. For statistical analyses, means were compared across genotypes using a one-way analysis of variance (ANOVA) and JMP Pro 15 Software (JMP®, Version *15*. SAS Institute Inc., Cary, NC, 1989–2021). We checked for the normality of the data by examining the normal quantile plot of their residuals. P-values less than 0.05 were considered statistically significant.

To quantify the number of *Sox2* stem cells, 40x confocal images of the dorsal nasal septal sections were obtained using a Zeiss LSM800 microscope as described above. For this analysis, we obtained a 5 μm thick section from a range of z-stacks (10-15 μm). Similar to our GAP43 analysis, we placed a rectangle along the OE and counted the number of immunoreactive cells within that defined region. The number of Sox2-labeled cells was averaged from two sections/mouse and the mean was obtained. We analyzed *OMP-cre*; *Dab1 f/+* (n= 4), *OMP-cre*; *Dab1 f/f* (n= 5), and no-cre control groups (no-cre; *Dab1 f/+;* no-cre; *Dab1 f/f;* n= 5). Statistical analyses were performed using the same methods described above.

To quantify the number of Ki67-labeled cells, 40x confocal images of the dorsal nasal septum were obtained using a Zeiss LSM800 microscope as described above. For this analysis, we obtained 5 μm sections from a range of z-stacks (10-15 μm). Similar to our GAP43 analysis, we placed a rectangle along the OE and counted the number of immunoreactive cells within that

defined region. The number of *Ki67*-labeled cells were averaged from two sections/animal was obtained. For our *Ki67* analysis we had a sample size (n=3-4). We analyzed *OMP-cre*; *Dab1 f/+* (n= 4), *OMP-cre*; *Dab1 f/f* (n= 3), and no-cre control groups (no cre; *Dab1 f/+;* no cre; *Dab1 f/f;* n= 4). Statistical analyses were conducted as described above.

Results:

Genetic labeling of OMP is consistent with OMP immunohistochemistry, with few differences

It is well established that OMP is expressed by mature OSNs throughout the olfactory epithelium (Farbman and Margolis, 1980). To determine if the pattern of genetic OMP expression matches our localization of OMP immunohistochemistry before analyzing the conditional Dab1-cre line, we compared these two techniques in 4 pairs of *OMP-cre, Ai14* and no-cre; *Ai14*. When we compared the pattern of the genetically labeled Td-Tomato (Td-Tom)-labeled cells in *OMP-cre* (Fig. 1A,C) mice with those identified by OMP protein localization (Fig. 1 A,B). The two single channel images look similar (Fig. 1B,C). When merged in figure 1A, however, there are differences in expression levels of axon bundles in the olfactory nerve, as some regions display co-expression and others primarily contain TdTom or OMP immunofluorescence (Figs. 1A, 2A). There are regions along the OE where TdTom was expressed at low levels compared to other TdTom-expressing OSNs that express higher levels (Fig. 2A). In addition, some, but not all, of the sustentacular cells are distinctly labeled by the OMP genetic marker (Fig. 2A,C: yellow arrows) and not labeled by the OMP immunohistochemistry (Fig. 2A,C) as mentioned by Li *et al.,* (2004). Overall, TdTom was a faithful representation of OMP expression in the OE (Fig. 1).

Many immature OSNs exclusively express GAP 43, but a few coexpress OMP

In order to determine if GAP43 expression is limited to immature OSNs in the OE, we compared its expression to the strong levels of TdTom in mature OSNs. The GAP43-labeled immature OSNs are found in the basal olfactory epithelium directly adjacent to the stem cells, and form a distinct green band. Confocal images show that the majority of OSNs express OMP or GAP43 exclusively (Fig. 3A-C); there are, however, some OSNs that express both proteins (white arrowheads). We suggest that these maybe OSNs that are transitioning from immature to mature OSNs.

Conditional deletion of *Dab1* reduces the immature OSNs in the OE compared to controls.

We generated a conditional deletion of *dab1* in OMP-expressing cells to examine the role of Dab1 within the OE. Initially we asked if the deletion of *Dab1* would alter the number of immature OSNs that express GAP43. We sampled a defined region of the nasal septum (72 μm by 414 μm rectangle) along the dorsal nasal septum in anterior (Fig. 4A) and posterior (Fig. 4B) sections of the 4 ODA genotypes (Fig. 4A,B). GAP 43-immunolabeled cells were counted from four sections/mouse by 2 investigators. Our quantitative analysis showed that the mean number of OSNs in the no-cre; *Dab1* f/+ (58 $\pm$ 2.7 neurons) and no-cre *Dab1f/f* (53 $\pm$ 7.4 neurons) controls did not differ and therefore were combined. There were fewer GAP43-labled OSNs in the *OMP-cre; Dab1 f/f* (42 $\pm$ 4.2) mice compared to the controls (56 $\pm$ 3.7 neurons). The number of OSNs in the *OMP-cre; Dab1 f/+* (50 $\pm$ 4.6) did not differ from the controls (Fig. 5 A-D). This decrease in GAP43-labeled OSNs observed following the *Dab1* deletion implies that Dab1 expression has a role in OSN neurogenesis.

Compared to controls, *Dab1* deletion in OSNs severely reduces *Sox2*-expressing olfactory progenitor cells.

Once we determined there was a difference in the number of immature OSNs in our *dab1* conditional mice, we next asked whether the GBC stem cells that generate OSNs also exhibited a reduction. We identified the total number of GBCs marked with Sox2 immunoreactivity, and conduced the same analysis as described above. The number of Sox2-positive cells was counted from two sections/mouse, and then the mean was obtained. Our analysis showed that the average number of *Sox2*-labeled cells in the *OMP-cre*; *Dab1 f/+* (8 $\pm$ 3 neurons) and no-cre control group (14 $\pm$ 2.7) did not differ between genotypes. In contrast, the number of *Sox2*-expressing stem cells in *OMP-cre; Dab1 f/f* mice (2 $\pm$ 2.7) were low in comparison to the no-cre control group (14 $\pm$ 2.7; Fig. 6 A-E.; p= 0.0121). The reduction in the number of stem cells when *dab1* is deleted suggests that the loss of Dab1 could lead to reduced cell turnover in the OE.

Conditional *Dab1* deletion greatly reduces the number of Ki67-expressing cells compared to controls.

To study differences in the number of actively proliferating cells in the OE, we performed immunohistochemistry for Ki67, and performed the same analysis used for our analysis of Sox2-labeled stem cells. The Ki67-labeled cells are located along the basement membrane in OE section. We counted the Ki67-expressing cells in two samples/mouse, and obtained a mean number/animal. We did not see a difference in the number of Ki67-labelled cells between the *OMP-cre*; *Dab1* f/+ (13 $\pm$ 2.9 progenitor cells) and no-cre control group (17 $\pm$ 2.9 progenitor cells). Consistently, however, we found that the mean number Ki67-labeled cells in *OMP-cre; Dab1 f/f* (6 $\pm$ 3.3) mice was much lower than those found in the control group (Fig.

7A-E.; p= 0.0378). A conditional deletion of *dab1* in OSNs results in a reduction of proliferating cells in the OE.

Discussion

Although the function of Reelin is well studied in the brain, far less is known about its role in the olfactory system. Initially we compared both the genetic and immunohistochemical markers of OMP in OSNs, and saw that they were similar, except that TdTom labeled a number of sustentacular cells. We also found that immature OSNs are marked by GAP43 expression but identified a few immature OSNs that coexpressed low levels of OMP. To determine if the Reelin-signaling pathway influences adult neurogenesis in the OE, we generated a conditional deletion of *dab1* in OMP-expressing cells. We used GAP43 expression, a marker for immature OSNs, to assess differences in number of immature OSNs between genotypes. We found that the conditional *dab1* mutants (*OMP-cre*; *Dab1 f/f*) had fewer GAP43-labeled cells in the OE than the control group. Additionally, we quantified the number of olfactory progenitor cells and proliferating cells in the OE using *Sox2* and *Ki67*, respectively. We found that the conditional *dab1* mutants had a reduced number of *Sox2* and *Ki67*-labeled cells compared to their controls. These findings imply that the loss of *dab1* reduces OSN neurogenesis.

The loss of Dab1 reduces cell proliferation within the OE.

Reelin, its two receptors, ApoER2, and VLDLR, and Dab1 are expressed within the olfactory system during development and throughout adulthood in mice, but its function within this system is currently unknown. We found that Dab1 is highly expressed in the OSN axons, and that the axons are surrounded by Reelin-expressing OECs (unpublished data). To understand

the role of the Reelin-signaling pathway on olfactory function, we performed olfactory behavioral testing on *Dab1* and *Reeler* wild type and mutant mice. We found both *Dab1* and *Reeler* mutants had poor odor detection compared to their wild type mice (unpublished data). Although there are 2 or more synaptic connections between the OSNs and the olfactory cortex, we hypothesized that the selective loss of Dab1 expression only in OSNs would contribute to the loss of olfactory sensitivity in the *Dab1* and *Reeler* mutant mice.

Previously, *dab1* was shown to influence adult neurogenesis in the central nervous system, i.e., the subventricular zone and hippocampus (Kim et al., 2001; Andrade et al., 2007; Teixeira et al, 2012). Although *dab1* has been implicated in modulating CNS adult neurogenesis, there is no current evidence of its role in the PNS, which contains the largest neurogenic region — the OE. Our findings that a deletion of *dab1* in OMP-expressing cells resulted in a reduction of olfactory stem cells and immature OSNs parallels previous work showing that the loss of dab1 disrupts adult neurogenesis in the CNS.

Our findings suggest that the loss of *dab1* contributed to a robust loss of olfactory stem cells but only a modest decrease of GAP43-labled immature OSNs. A potential explanation for these findings is that not many olfactory stem cells are required to maintain OSNs turnover. The loss of *dab1* reduced the number of olfactory stem cells and immature neurons; however, the functional impact of this reduction remains unclear.

Decreases in olfactory sensitivity is not solely due to a reduction in OSNs.

In addition to characterizing differences in proliferation in the OE, we are performing olfactory behavioral analyses on our ODA groups. Based on our preliminary data, we do not see a significant difference in the sensory detection in our conditional *dab1* mutant or heterozygous

mice. These results suggest that although the loss of Dab1 results in fewer olfactory stem cells and immature OSNs, enough of the OSNs are contacting the mitral cells in the glomeruli to maintain both attractive and aversive sensory function. Additional regions within the olfactory pathway will need to be examined to compare changes associated with sensory loss found in the *Reln* $^{-/-}$ and *Dab1*$^{-/-}$ mice.

Olfaction requires communication between both the peripheral and central nervous system to correctly identify various odorants. The focus of this study has specifically examined the Reelin-signaling pathway within the peripheral nervous system. However, substantial Reelin and Dab1 are present within the olfactory bulb, associated olfactory areas, and in the olfactory cortex (Hack *et al.*, 2002). The OSN axons project to and synapse in their specific glomerular targets on dendrites of the Reelin-expressing mitral cells. The axons of the mitral cells then converge forming the olfactory tract which projects to the piriform cortex, anterior olfactory nucleus, and amygdala. The piriform cortex receives the largest number of direct olfactory bulb projections and plays a significant role in deciphering olfactory input (Stettler and Axel, 2009). The piriform cortex is a three-layered structure, with the second layer composed of numerous Reelin-positive cells. Carceller et al. (2016) found that the *Reeler* mutants have lamination defects in their piriform cortex. This alteration in the piriform cortex would likely contribute to the loss of olfactory sensitivity found in the *Reln* and *Dab1* mutants but not in our ODA mutants. Future studies should analyze differences in the piriform cortex to determine if these cortical structures are responsible for the olfactory deficiency observed in the *Reln* and *Dab1* mutants.

Figures

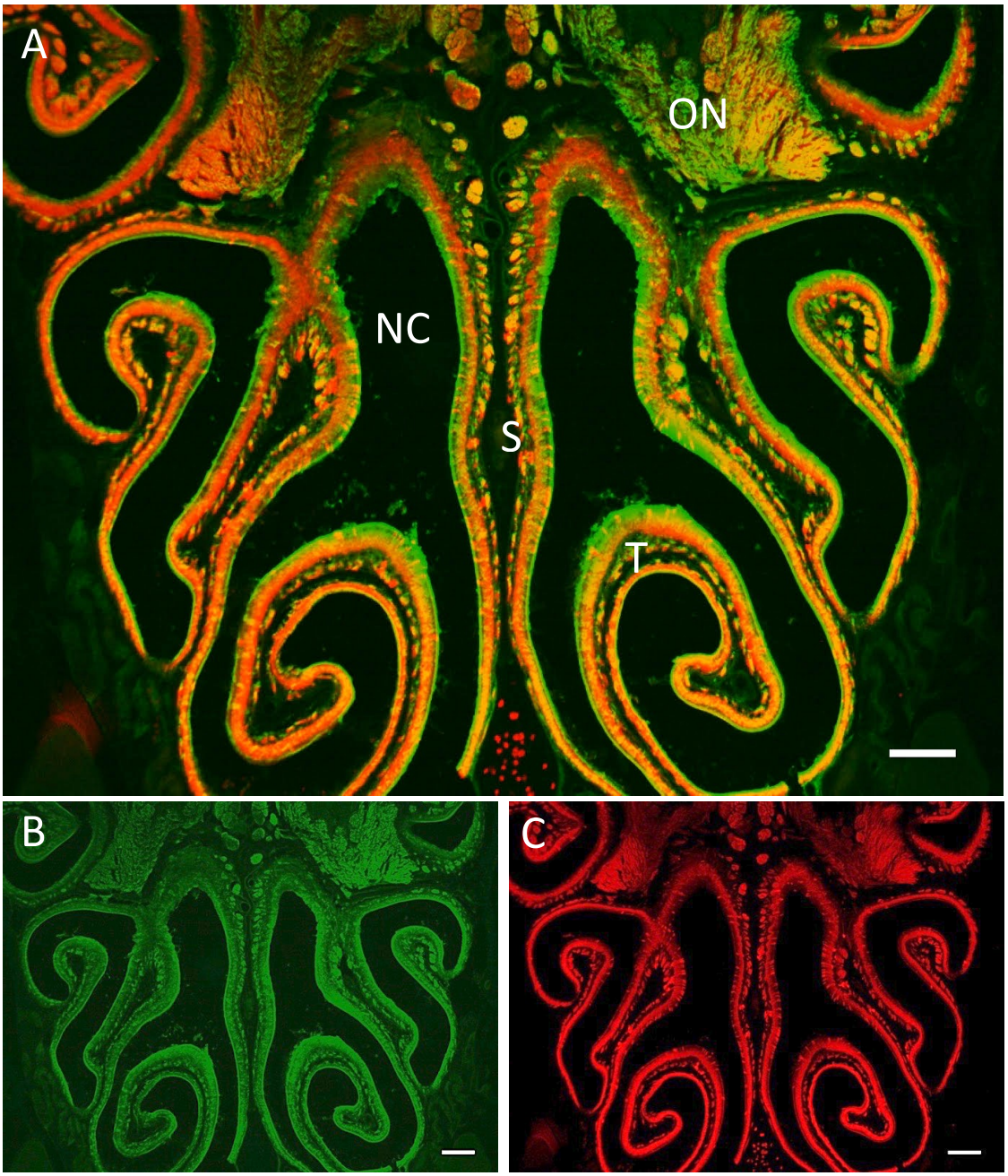

Figure 1: Mature OSNs are marked by TdTomato and OMP immunohistochemistry in a coronal section of the olfactory epithelium. The nasal cavity of an *OMP-cre; Ai14* mouse is oriented with the rostral towards the top. A. OMP immunohistochemistry (green) and TdTomato Reporter (red) show the OSN axons forming the olfactory nerve (ON) fascicles that project toward the cribriform plate. Some olfactory nerve fascicles appear to contain mainly TdTom or green immunolabeled axons. B. Single channel of OMP immunohistochemistry (green) C. Single channel of TdTomato reporter. S: septum, NC: nasal cavity, T: turbinates, ON: olfactory nerve. Scale bars A-C = 50 μm.

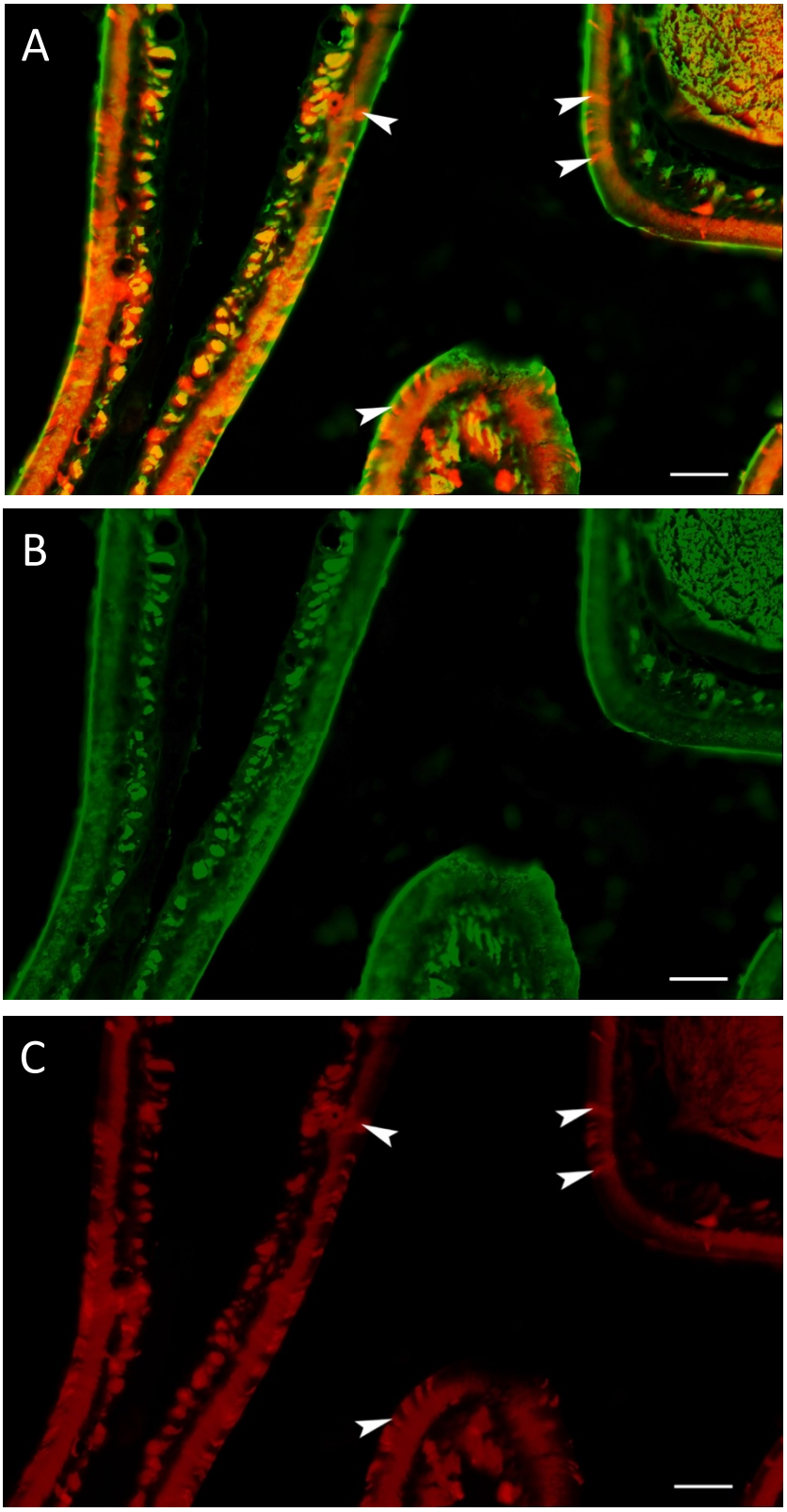

Figure 2: Differential expression of both TdTomato and OMP immunofluorescence in mature OSNs. Coronal section of olfactory epithelium (*OMP-cre; Ai14*). A. TdTomato reporter (red) and OMP immunoreactivity (green) in the apical olfactory epithelium with rostral toward the left. OMP-labeled axons do completely overlap with TdTomato immunoreactivity as seen in large nerve bundles on the right. TdTomato marks some Sustentacular cells (white arrowheads); B. Single channel of OMP immunohistochemistry (green), C. Single channel of TdTomato reporter (red). Scale bars = 100 μm.

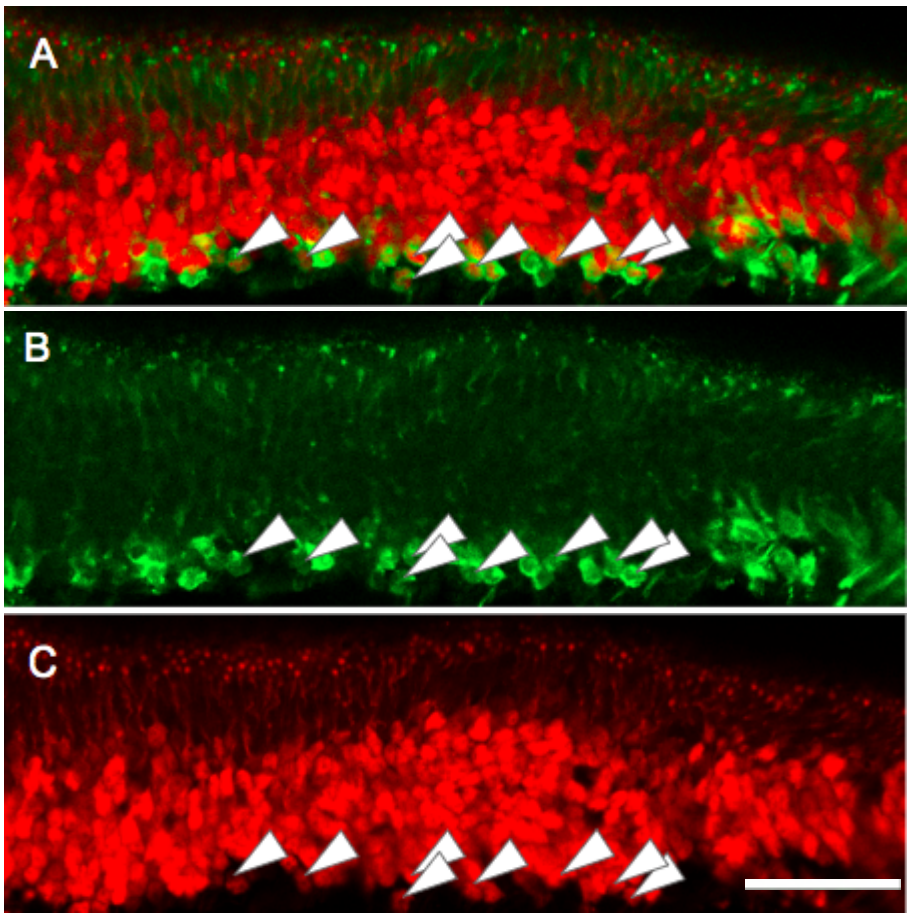

Figure 3: Mature OSNs in the olfactory epithelium express TdTomato while immature OSNs are marked by GAP43. A. Coronal section of olfactory epithelium (*OMP-cre*; *Ai14*) shows expression of TdTomato (red) and GAP43 (green) in the cilia and dendritic knobs along the apical layer. TdTomato marks cell bodies in the more apical layer, whereas GAP43 expression marks cell bodies in the basal layer of the olfactory epithelium. A small number of cells express both OMP and TdTom (arrowheads). B. Single channel of GAP43 immunoreactivity that mark immature OSNs; C. Single channel for TdTomato marks mature OSNs. Scale bar A-C = 50 μm.

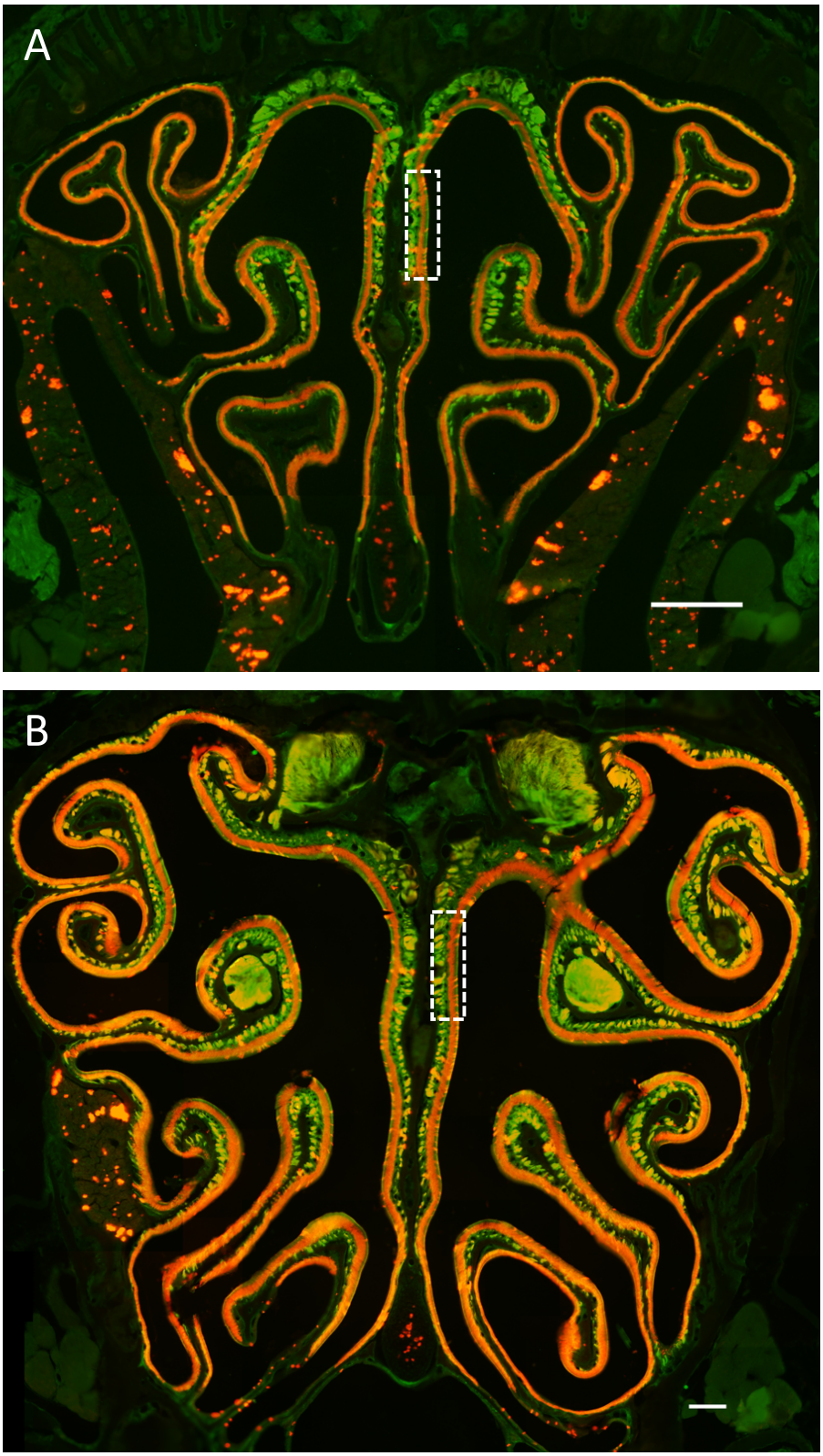

Figure 4: The septum provides a consistent region to sample GAP43, Sox2, and Ki67 expression in the olfactory epithelium (OE) Anterior (A) and posterior (B) coronal sections (*OMP-cre; Ai14*) were used to sample the OE within the rectangle box.
Scale bars A,B = 100 µm.

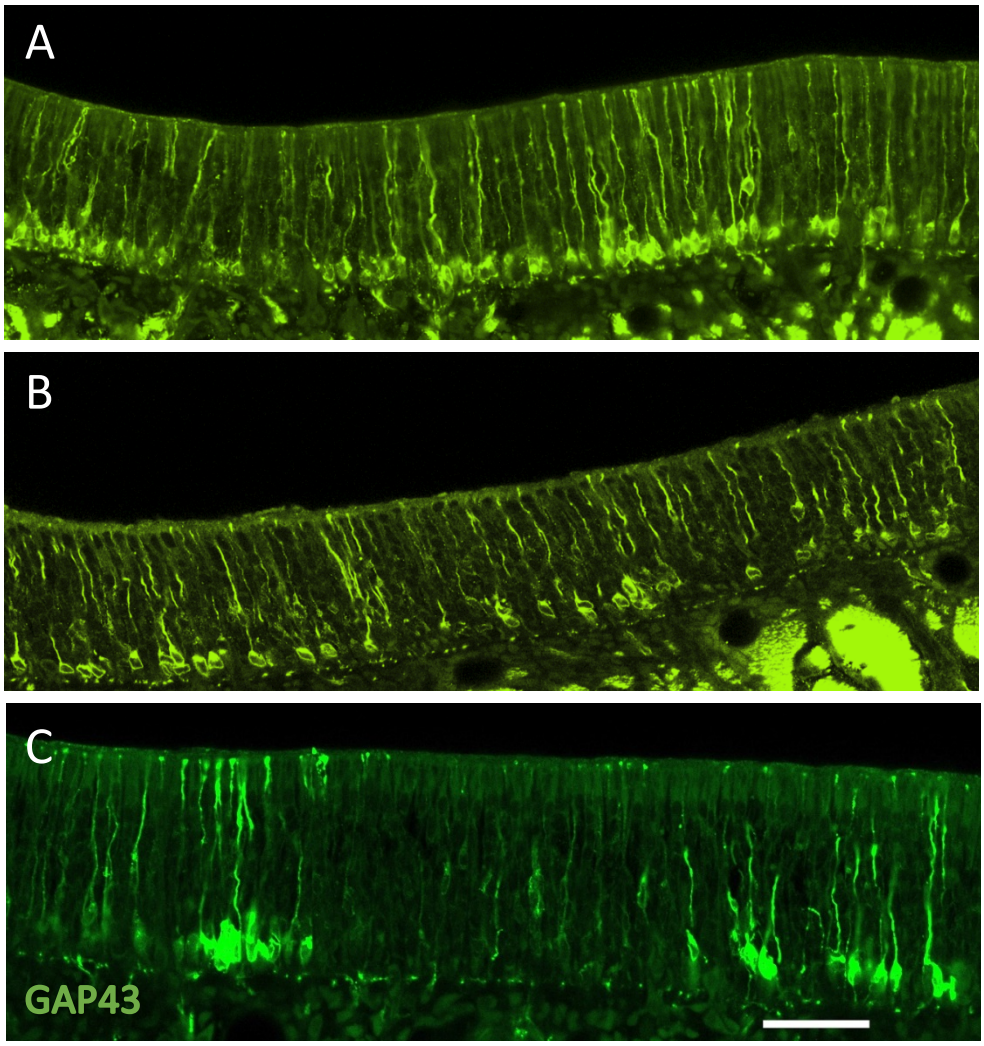
A
B
C
GAP43

D

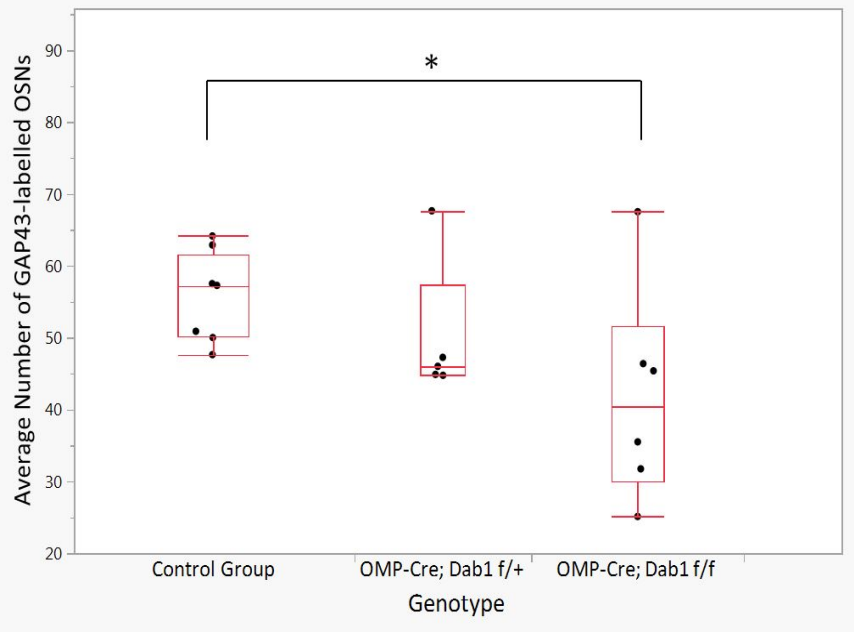
Average Number of GAP43-labelled OSNs
90
80
70
60
50
40
30
20
*
Control Group
OMP-Cre; Dab1 f/+
OMP-Cre; Dab1 f/f
Genotype

Figure 5: *OMP-cre; Dab1 f/f* mice have fewer GAP43-labeled OSNs compared to their control groups. A-C. Coronal sections of OE represents the boxed sample analyzed from each ODA genotype: no-cre controls (A), *OMP-cre; Dab1f/+* (B), and *OMP-cre; Dab1f/f* (C). There appear to be fewer GAP43-expressing OSNs in *OMP-cre; Dab1f/f* (C) compared to the no-cre controls (A). D. Quantitative analyses show that the *OMP-cre; Dab1 f/f* mice (42 $\pm$ 4.6 neurons; n= 6) have a reduced average number of immature OSNs compared the control group (56 $\pm$ 3.7 neurons; n= 8) and *OMP-cre; Dab1f/+* (50 $\pm$ 4.7 neurons; n= 5) mice. The number of OSNs in the *OMP-cre*; *Dab1* f/+ did not differ from the controls. Scale bar A-C = 50 μm.

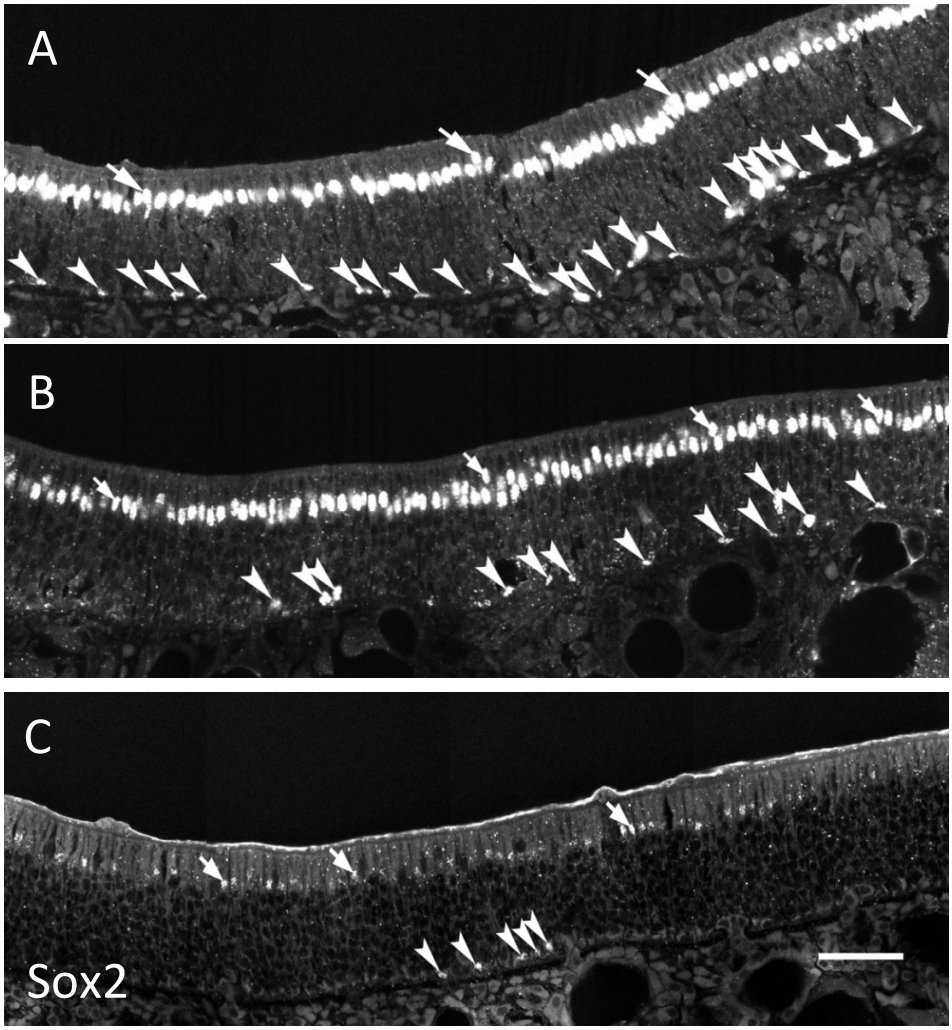
A
B
C
Sox2

D

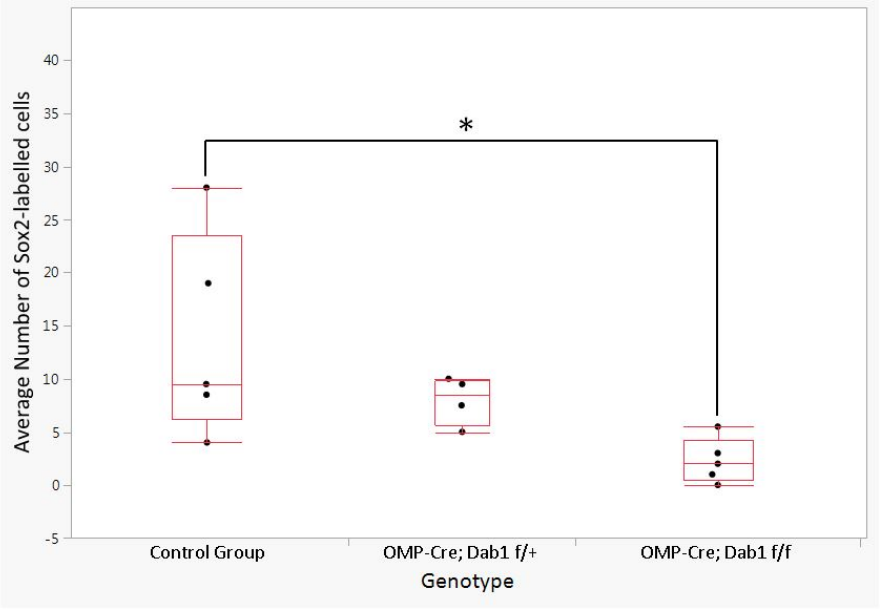
Average Number of Sox2-labelled cells
40
35
30
25
20
15
10
5
0
-5
*
Control Group
OMP-Cre; Dab1 f/+
OMP-Cre; Dab1 f/f
Genotype

Figure 6: *OMP-cre; Dab1 f/f* mice have fewer Sox2-labeled olfactory stem cells than the control groups. A-C. Coronal sections of olfactory epithelium show Sox2-labeled olfactory stem cells in the basal portion of the epithelium (arrowheads) and sustentacular cells (arrows) in the apical edge of the epithelium in no-cre controls (A), *OMP-cre; Dab1f/+*(B), and *OMP-cre; Dab1f/f* (C). D. The statistical analysis shows that the *OMP-cre*; *Dab1 f/f* mice (2 $\pm$ 2.7 cells; n= 5) had fewer Sox2-positive olfactory stem cells compared the control group (14 $\pm$ 2.7 cells; n= 5, p= 0.0121). The average number of Sox2-labeled cells did not differ between the *OMP-cre*; *Dab1* f/+ (8 $\pm$ 3 neurons) and no-cre control group. Scale bar A-C = 50 μm.

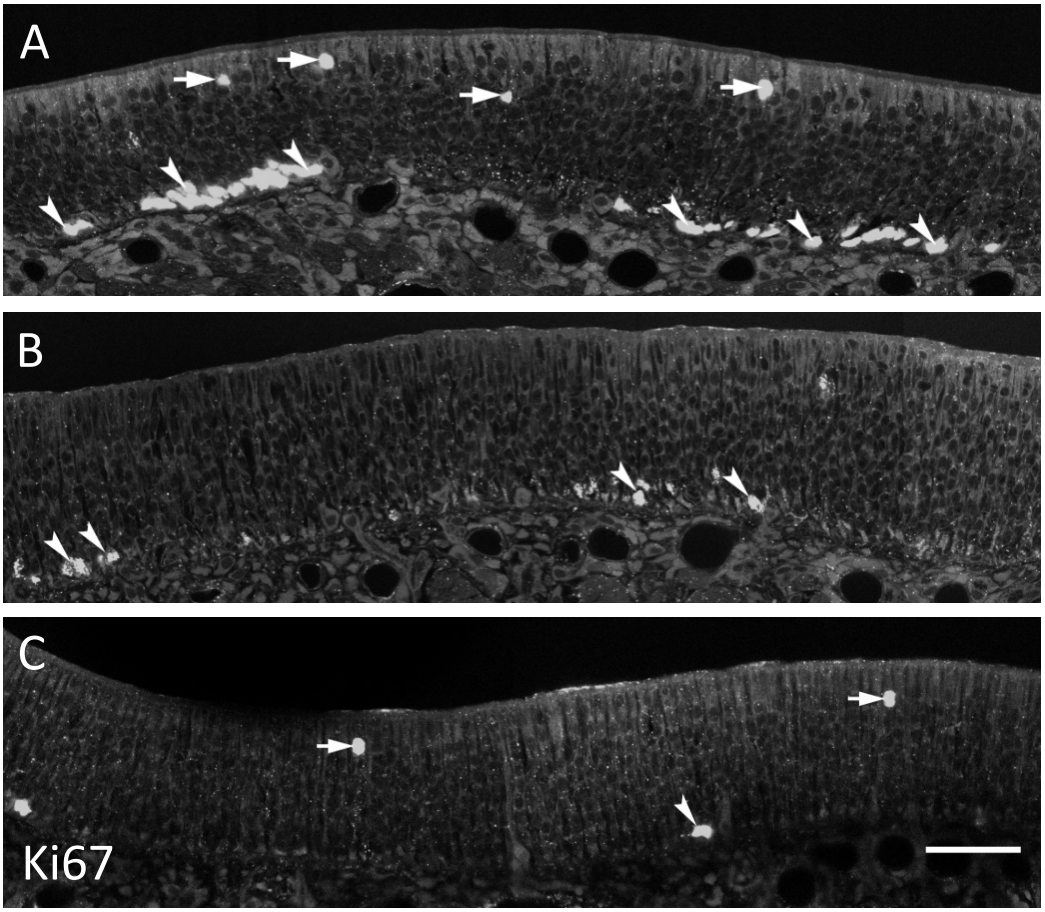
A
B
C
Ki67

D

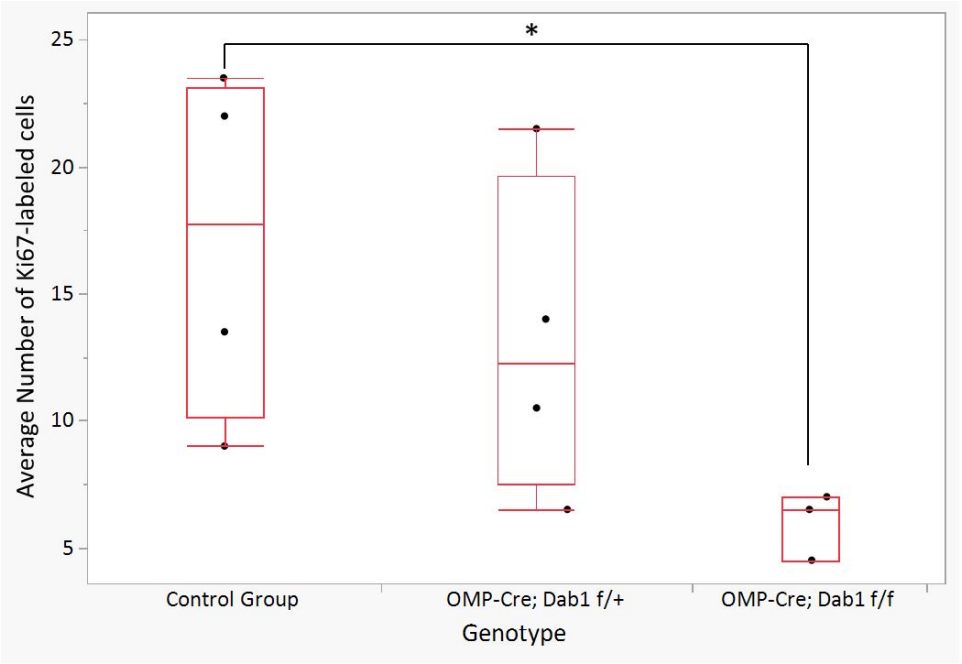
*
25
20
15
10
5
Average Number of Ki67-labeled cells
Control Group
OMP-Cre; Dab1 f/+
OMP-Cre; Dab1 f/f
Genotype

Figure 7: *OMP-cre; Dab1* f/f mice have fewer *Ki67*-labeled proliferating olfactory stem cells in comparison to the control group. (A-C) Ki67 immunoreactivity labels any proliferating stem cells (arrowheads) in the OE of no-cre controls (A), *OMP-Cre; Dab1 f/+* (B) and *OMP-cre; Dab1 f/f* (C) mice. Anti-Ki67 also labels any proliferating cell in the OE, including the sustentacular cells (arrows). D. *OMP-cre; Dab1 f/f* mice (6 $\pm$ 3.3; n= 3) had far fewer Ki67-labled cells in the OE than the controls (17 $\pm$ 2.9; n= 4, p= 0.0378). There was not a significant difference in the number of Ki67-labeled cells when comparing the *OMP-Cre; Dab1 f/+* (13 $\pm$ 2.9; n= 4) to the no-cre control group or the *OMP-cre*; *Dab1 f/f* mice. Scale bar A-C = 50 μm.

Primary Antibody	Source, catalog no.	Species	Antibody concentration	Amplification	Source, catalog no.
GAP43	Abcams, ab16053	Rabbit	1:500	Donkey anti-Rabbit-488	Thermo Fisher Scientific, 2256732
OMP	FujifilmWako, 544-10001-WAKO	Goat	1:1000	Donkey anti-Goat-555	Jackson ImmunoResearch, 124775
Sox2	Abcams, ab92494	Rabbit	1: 5000	Tyramide signal amplification	Perkin Elmer LLC, NEL741001KT
Ki67	Abcams, ab16667	Rabbit	1: 5000	Tyramide signal amplification	Perkin Elmer LLC, NEL741001KT

Table 1: Summary of primary and secondary antibodies used in our analyses of the olfactory epithelium.

References

Alcantara S, Ruiz M, D'Arcangelo G, Ezan F, de Lecea L, et al. (1998) Regional and cellular patterns of reelin mRNA expression in the forebrain of the developing and adult mouse. J Neurosci 18: 7779–7799.

Buck L, Axel R (1999) A novel multigene family may encode odorant receptors: A molecular basis for odor recognition. Cell 65:175-187.

Carter LA, MacDonald JL, Roskams AJ (2004) Olfactory horizontal basal cells demonstrate a conserved multipotent progenitor phenotype. J Neurosci 24:5670-5683.

Cau E, Gradwohl G, Fode C, Guillemot F (1997) Mash1 activates a cascade of bHLH regulators in olfactory neuron progenitors. Development 124:1611–1621.

Chess A, Simon I, Cedar H, Axel R (1994) Allelic inactivation regulates olfactory receptor gene expression. Cell 78: 823-834.

Clowney EJ, LeGros MA, Mosley CP (2012) Nuclear aggregation of olfactory receptor genes governs their monogenic expression. Cell 151:724–737.

D'Arcangelo G, Homayouni R, Keshvara L, Rice DS, Sheldon M, Curran T (1999) Reelin is a ligand for lipoprotein receptors. Neuron 2:471-479.

Dairaghi L, Flannery E, Giacobini P, Saglam A, Saadi H, Constantin S, Casoni F, Howell BW, Wray S (2018) Reelin can modulate migration of olfactory ensheathing cells and gonadotropin releasing hormone neurons via the canonical pathway. Frontiers in Cellular Neuroscience. 12:228.

Farbman A, Margolis F (1980) Olfactory marker protein during ontogeny: Immunohistochemical localization. Developmental Biology 74:205-215.

Gerdes J, Lemke H, Baisch H, Wacker HH, Schwab U, Stein H (1984) Cell cycle analysis of a cell proliferation-associated human nuclear antigen defined by the monoclonal antibody Ki-67. J Immunology. 133:1710-1715.

Hack I, Bancila M, Loulier K, Carroll P, Cremer H. (2002) Reelin is a detachment signal in tangential chain-migration during postnatal neurogenesis. Nat Neurosci 5:939–945.

Holbrook EH, Szumowski KE, Schwob JE (1995) An immunochemical, ultrastructural, and developmental characterization of the horizontal basal cells of rat olfactory epithelium. J Comp Neurol. 363:129-46.

Howell BW, Herrick TM, Cooper JA (1999) Reelin-induced tyrosine [corrected] phosphorylation of disabled 1 during neuronal positioning. Genes Dev.13:643-64

Howell BW, Gertler, FB, Cooper, JA (1997) Mouse disabled (mDab1): a Src binding protein implicated in neuronal development. EMBO J. 16:121–132.

Huard JM, Schwob JE (1995) Cell cycle of globose basal cells in rat olfactory epithelium. Dev Dyn: 203:17-26.

Li J, Ishii T, Feinstein P, Mombaerts P (2004) Odorant receptor gene choice is reset by nuclear transfer from mouse olfactory sensory neurons. Nature 428:393-399.

Kim HM, Qu T, Kriho V, Lacor P, Smalheiser N, et al. (2002) Reelin function in neural stem cell biology. Proc Natl Acad Sci U S A 99: 4020–4025.

Klenoff JR and Greer CA (1998) Postnatal development of olfactory receptor cell axonal arbors. J. Comp. Neurol: 390:256-267.

Leung CT, Coulombe PA, Reed RR (2007) Contribution of olfactory neural stem cells to tissue maintenance and regeneration. Nat Neurosci.10:720–726.

Liberia T, Martin-Lopez E, Meller S, Greer C (2019) Sequential Maturation of Olfactory Sensory Neurons in the Mature Olfactory Epithelium. eNeuro 6(5):ENEURO.0266-19.

Mackay-Sim A, Kittel P (1991) Cell dynamics in the adult mouse olfactory epithelium: a quantitative autoradiographic study. J Neurosci: 11:979-84.

Manglapus GL, Youngentob SL, Schwob JE (2004) Expression patterns of basic helix-loop-helix transcription factors define subsets of olfactory progenitor cells. J Comp Neurol. 479:216-33.

Mombaerts, P (2001) How smell develops. Nature Neurosci. 4(Suppl.):1192–1198.

Monti Graziadei GA, Graziadei PP (1979) Neurogenesis and neuron regeneration in the olfactory system of mammals. II. Degeneration and reconstitution of the olfactory sensory neurons after axotomy. J Neurocyto., 8:197–213

Nicolay DJ, Doucette JR, Nazarali AJ (2006) Transcriptional regulation of neurogenesis in the olfactory epithelium. Cell Mol Neurobiol. 26:803-821.

Packard A, Schnittke N, Romano RA, Sinha S, Schwob JE (2011) DeltaNp63 regulates stem cell dynamics in the mammalian olfactory epithelium. J Neurosci. 31:8748-8759.

Rice D S, Sheldon M, D'Arcangelo G, Nakajima K, Goldowitz D, Curran T (1998) Disabled-1 acts downstream of Reelin in a signaling pathway that controls laminar organization in the mammalian brain. Development 125:3719– 3729.

Roskams AJ, Cai X, Ronnett GV (1998) Expression of neuron-specific beta-III tubulin during olfactory neurogenesis in the embryonic and adult rat. Neuroscience 83:191–200

Schnaufer C, Breer H, Fleischer J (2009) Outgrowing olfactory axons contain the Reelin receptor VLDLR and navigate through the Reelin-rich cribriform mesenchyme. Cell and tissue research. 337:393-406.

Schwob JE, Jang W, Holbrook EH, Lin B, Herrick DB, Peterson JN, Hewitt Coleman J (2017) Stem and progenitor cells of the mammalian olfactory epithelium: Taking poietic license. J Comp Neurol. 525:1034-1054.

Strittmatter S, Fankhauser, Huang CP (1995) Neuronal pathfinding is abnormal in mice lacking the neuronal growth cone protein GAP-43. Cell 80: 445-452.

Verhaagen J, Oestreicher A, Gispen WH, Margolis F L (1989) The expression of the growth associated protein B50/GAP43 in the olfactory system of neonatal and adult rats. J Neurosci 9:683–691.

Wyss JM, Stanfield BB, Cowan WM (1980) Structural abnormalities in the olfactory bulb of the Reeler mouse. Brain Research 188: 566–571.